

# Design and Implementation of PSO Based LQR Control for Inverted Pendulum through PLC

Suppachai Howimanporn, Sunphong Thanok, Sasithorn Chookaew, and Warin Sootkaneung, *Member, IEEE*

**Abstract**— This work proposes design and implementation of an optimal inverted pendulum controller using linear quadratic regulator (LQR) based on particle swarm optimization (PSO). The LQR feedback module is implemented on the Mitsubishi Q series-UDV programmable logic controller (PLC). In this paper, the optimum gains of the PSO based LQR are predefined offline by MATLAB and subsequently, evaluated in our experimental inverted pendulum. The results show that our proposed PSO based LQR technique provides the maximum swing with as low as 4 times of that from the traditional LQR approach when applied to the real plant.

## I. INTRODUCTION

Since an inverted pendulum represents a multivariable nonlinear system that is highly vulnerable to instability, balancing control of the inverted pendulum has been considered as an important research area in control engineering. A number of studies have explored efficient methods to stabilize inverted pendulum systems. PID based techniques have been developed to balance the inverted pendulum under the linear approximation of the system [1]. Sliding mode control (SMC) algorithm has been adopted into position control of the inverted pendulum system with nonlinear consideration [2]. However, both PID and SMC based approaches may not suitable for multiple-input, multiple-output (MIMO) systems [3]. Linear quadratic regulator LQR outperforms others because it can perform well for nonlinear MIMO systems [4]. In LQR algorithm, the performance index function of LQR, which is known as the cost function, depends upon selection of the weight matrices and time duration. In most previously proposed methods, the final time is assumed infinitely long and the optimal gain  $K$  of the LQR can be obtained from the Riccati algebraic equation. Yet, determination of this optimal gain for finite time duration is rather difficult. For this reason, particle swarm optimization (PSO), which is suitable for searching

for the solution within limited time duration, is selected in our work.

PSO is an evolutionary algorithm which was developed in 1995 by Kennedy and Eberhart [5]. The algorithm is derived from motion of swarm or flock of animals; e.g. birds, fish. The PSO mimics the behavior of individuals in a swarm to maximize the survival of the species. PSO can be used to solve optimization problems by cooperation and competition among the individuals based on iterations. The algorithm keeps the global search strategy based on the entire swarm, and avoids complex operations. Due to its simple definition, easy implementation, strong convergence, and robustness, PSO is attractive for solving nonlinear problems. Many research studies on applications of PSO in various control systems have been proposed. A linear state feedback controller based on the linearized inverted pendulum model is considered in [6, 7]. Comparisons of accuracy and computational efficiency between two of the evolutionary algorithms, GA and PSO, were investigated in [8 - 12]. Those studies reveal that PSO solves the optimal results faster than GA.

In this work, we employ LQR to stabilize the Inverted pendulum system. We also use PSO to determine the optimal gain of the LQR under finite time duration of the cost function. The result of optimal gain from the proposed method is evaluated through simulation and real inverted pendulum plant. In the physical system, the predefined gains of LQR from different approaches are inserted into corresponding PLC instructions to compare the performance of those algorithms. Experimental results show that the proposed PSO based LQR can provide more attractive outcome than previous techniques.

The rest of this paper is organized as follows. Sections II and III provide a background of inverted pendulum systems and the proposed design technique, respectively. Section IV discusses the results and interesting remarks. Finally, section V gives the conclusion of this work.

## II. INVERTED PENDULUM SYSTEM

A single-axis inverted pendulum system developed in this work to evaluate the proposed control algorithm is shown in Figure 1. The pendulum rod has 1.00 cm-diameter, and 1.0 m-length. The entire system is supported by a platform with the weight of 30.0 kg and the length of 150 cm. The balancing movement is driven by a 24 V, 350 W, 3000 RPM-DC motor. A set of encoder sensors are connected to measure the angle and position of the pendulum. The Mitsubishi Q series-UDV PLC is used as the main controller for the system which supports most of the required functions; e.g., PWM, feedback measurement, and ADC/DAC.

Manuscript received August 12, 2016. This work was supported in part by the Department of Teacher Training in Mechanical Engineering, Faculty of Technical Education, King Mongkut's University of Technology North Bangkok.

S. Howimanporn is with the Faculty of Technical Education, King Mongkut's University of Technology North Bangkok, Thailand. (corresponding author's phone: 668-901-84049; fax: 662-586-9015; e-mail: suppachai.h@fte.kmutnb.ac.th)

S. Thanok is with the Faculty of Technical Education, King Mongkut's University of Technology North Bangkok, Thailand (e-mail: sunphong.t@fte.kmutnb.ac.th).

S. Chookaew is with the Faculty of Industrial Education, Rajamangala University of Technology Phra Nakhon, Bangkok, Thailand (e-mail: sasithorn.c@rmutp.ac.th)

W. Sootkaneung is with the Faculty of Engineering, Rajamangala University of Technology Phra Nakhon, Bangkok, Thailand (e-mail: warin.s@rmutp.ac.th)

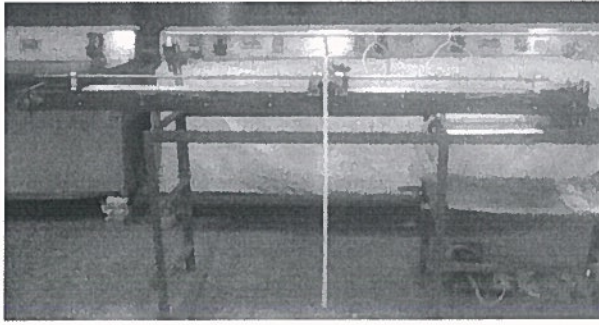


Figure 1. Inverted pendulum system photograph

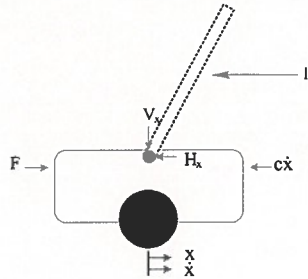


Figure 2. Free body diagram of inverted pendulum

Dynamics model for the Inverted pendulum system required in designing the controller is shown in Figure 2. A cart with the mass  $M$  is moved by the horizontal force  $u(t)$  from the motor. On the cart, an inverted pendulum with the mass  $m$  is attached via a frictionless hinge. The center of mass of the inverted pendulum locates at a distance  $l$  from the hinge end. The moment of inertia about the center of mass is denoted by  $I$ . The point of support of the pendulum is at the coordinate  $x(t)$  with respect to the world reference frame.  $\theta(t)$  is the angle of the inverted pendulum measured from the vertical axis.

From the free body diagram as shown in Figure. 2, we apply the Newton's second law of motion to the cart and obtain

$$\sum \vec{F} = m\vec{a} \quad (1)$$

$$\ddot{x} = \frac{1}{(m_c + m)} ml(\dot{\theta}^2 S\theta_1 - \ddot{\theta} C\theta) - c\dot{x} + F \quad (2)$$

$$\ddot{\theta} = \frac{1}{(I + ml^2)} ml(gS\theta - \ddot{x}C\theta) - b\dot{\theta} \quad (3)$$

Transfer functions can be obtained after taking Laplace transformation on the above equations. That is

$$\frac{\theta(s)}{u(s)} = \frac{\frac{ml}{JM} s}{(1 - \frac{m^2 l^2}{JM}) s^3 + (\frac{Jc + bM}{JM}) s^2 - \frac{(mMgl)}{JM} s - \frac{mglc}{JM}} \quad (4)$$

$$A = \begin{bmatrix} 0 & 1 & 0 & 0 \\ 0 & \frac{-Jb_e}{J_e} & \frac{-m^2 l^2 g}{J_e} & \frac{mlb}{J_e} \\ 0 & 0 & 0 & 1 \\ 0 & 0 & \frac{mlb_e E}{J(m_c + m) - m^2 l^2} & \frac{-bM}{J(m_c + m) - m^2 l^2} \end{bmatrix} \quad (5)$$

$$Bu = \begin{bmatrix} 0 \\ \frac{JK_l}{J_e rR} \\ \frac{mlEK_l}{rR} \\ 0 \end{bmatrix} [u] \quad (6)$$

$$y_x = \begin{bmatrix} 1 & 0 & 0 & 0 \\ 0 & 0 & 1 & 0 \end{bmatrix} \begin{bmatrix} x \\ \dot{x} \\ \theta_1 \\ \dot{\theta}_1 \end{bmatrix} \quad (7)$$

Descriptions and Values of all parameters are given in Tables I and II, respectively.

TABLE I. PARAMETER DESCRIPTIONS

Symbol	Parameters
$m$	Mass at the center of gravity of the rod.
$m_c$	Mass at the center of gravity of the cart.
$l$	Distance from the center of gravity of the rod to the pivot point.
$I$	Moment of inertia of the rod at the center of gravity.
$x$	Displacement of the cart.
$\theta$	Rod angle from vertical axis
$c$	Viscous friction coefficient of the cart.
$b$	Viscous friction coefficient of the rod
V&H	Action forces on the shorter rod.
$g$	Gravitational acceleration.
$F$	Force on the cart.

TABLE II. PARAMETER VALUES OF THE INVERTED PENDULUM

Symbol	Parameters	
	Value	Unit
$m$	0.18	kg
$m_c$	3.5	kg
$l$	1	m
$I$	0.025	kg/m <sup>2</sup>
$b$	0.02	N.s/m
$g$	9.81	m/s <sup>2</sup>
$c$	0.1	N.s/rad

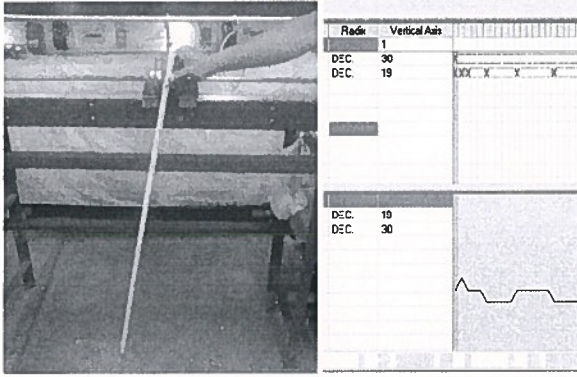


Figure 3. Encoder sensor measuring angle of inverted pendulum system

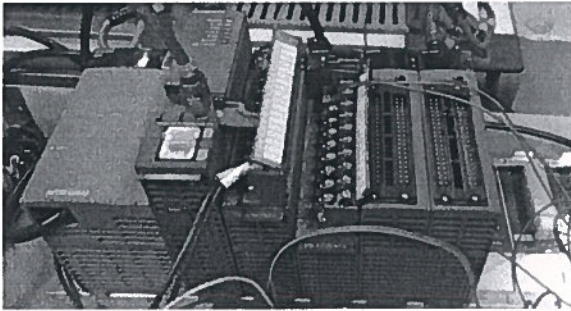


Figure 4. PLC module

Figure 3 shows data acquisition from two encoder sensors for position and angle measurement which are installed on the pendulum rod. In Figure 4, PLC module and related circuits are shown. We select the Mitsubishi Q series-UDV PLC for this work.

### III. CONTROLLER DESIGN

#### A. Linear Quadratic Regulator

State-space representation of the inverted pendulum is determined as

$$\dot{x} = Ax + Bu \quad (8)$$

$$x = [x \quad \dot{x} \quad \theta \quad \dot{\theta}]^T \quad (9)$$

$$y = cx \quad (10)$$

where  $x$  is the input matrix which contains position and angle and their speed.

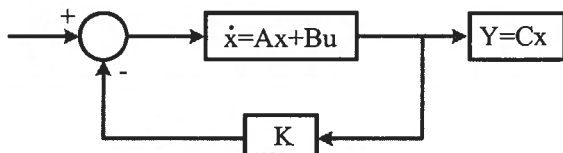


Figure 5. LQR block diagram

In LQR, the quadratic performance index function is defined as

$$J = \frac{1}{2} \int_0^{\infty} (x'(t) Qx(t) + u'(t) Ru(t)) dt \quad (11)$$

where the input  $u(t)$  is defined as

$$u(t) = -Kx(t) \quad (12)$$

where  $K$  is the optimal gain matrix. When the performance index function,  $J$ , is minimized,  $u(t)$  provides the optimal control signal. The objective of the design of optimal controller is to choose appropriate weighting matrices  $Q$  and  $R$  that reflect the importance of the relationship between the state error and control signal in the performance index function. Basically, the optimal gain of LQR for stable systems can be determined by solving an algebraic Riccati equation. However, as mentioned before, this is not efficient in computation time.

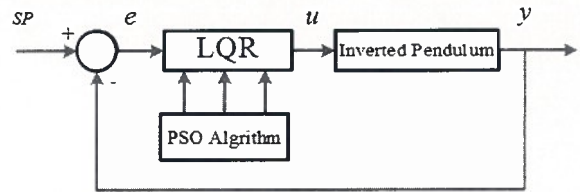


Figure 6. Diagram LQR controller for inverted pendulum

#### B. PSO Algorithm

We adopt PSO algorithm to search for the optimal gain of the LQR controller. In this work, PSO iteratively runs for 100 generations with population size of 40. The next velocity can be updated using the current velocity, the distance between the current position, the best previous position, and the distance between the current positions. The velocity for the current iteration can be evaluated as given in (13). In addition, the updated position can be calculated using (14)

$$v_{ij}^{k+1} = wv_{ij}^k + c_1r_1(pbest_{ij}^k - x_{ij}^k) + c_2r_2(gbest_{ij}^k - x_{ij}^k) \quad (13)$$

$$x_{ij}^{k+1} = x_{ij}^k + v_{ij}^{k+1} \quad (14)$$

$$\text{where } w = w_{\max} - \frac{w_{\max} - w_{\min}}{iter_{\max}} \times iter \quad (15)$$

where  $v_{ij}^{k+1}$  is the current speed of particle generation,  $v_{ij}^k$  is the speed of particle in the previous generation,  $r_1$  and  $r_2$  are random numbers,  $c_1$  and  $c_2$  are constants,  $x_{ij}^k$  is the current position,  $x_{ij}^{k-1}$  is the position of the particle in the previous generation,  $pbest_{ij}^k$  is an individual best solution,  $gbest_{ij}^k$  is the global best solution, and  $w$  is the inertia factor.

#### C. PSO based Optimal Gain LQR

The performance index (fitness or cost) function with finite time duration is represented by

$$J = \frac{1}{2} \int_0^{T_f} (x'(t) Qx(t) + u'(t) Ru(t)) dt \quad (11)$$

where  $T_f$  = final time .

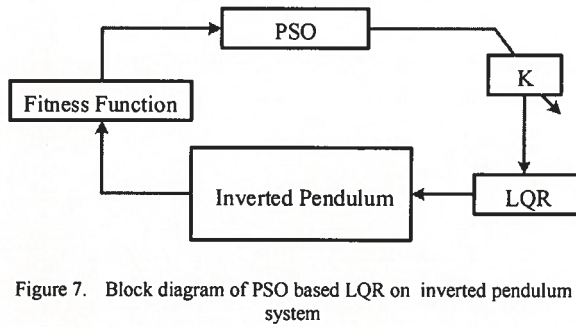


Figure 7. Block diagram of PSO based LQR on inverted pendulum system

Figure 7 shows a block diagram of PSO-based LQR for inverted pendulum system. Steps to design of PSO based LQR inverted pendulum balancing control are as follows.

1) Obtain mathematical models for the single-axis inverted pendulum. In this work, we assume that

$$A = \begin{bmatrix} 0 & 1 & 0 & 0 \\ 0 & -0.132 & -1.23 & 0.003 \\ 0 & 0 & 0 & 1 \\ 0 & 1.362 & 104.6 & -0.377 \end{bmatrix} \quad B = \begin{bmatrix} 0 \\ 0.03424 \\ 0 \\ -0.7236 \end{bmatrix}$$

2) Select the state and control weighting matrices  $Q$  and  $R$  in the fitness function.

$$Q = \begin{bmatrix} 5 & 0 & 0 & 0 \\ 0 & 1 & 0 & 0 \\ 0 & 0 & 10 & 0 \\ 0 & 0 & 0 & 1 \end{bmatrix} \quad R = 1$$

3) Initialize PSO with the value of fitness function, 40 random particles which are defined as the controller gains, 100 iterations, and  $T_f = 5$ .

4) Set local best,  $p_{best}$ , of each particle and determine global best,  $g_{best}$ , of the population.

5) Compare the global best with the target and check the iteration number to see whether the termination condition is met. If the termination criterion is met, go to step 7), otherwise continue to step 6).

6) Loop to step 4) (update the time iteration, particle's velocity ( $v$ ) and position ( $x$ ))

7) Choose the minimum global best,  $g_{best}$ , of the performance index function as the optimal gain  $K$ .

#### IV. EXPERIMENTAL RESULTS

With the iteration size of 100 and population size of 40, the values of global best of the performance index function is shown in Figure 8. It can be seen in this figure that at the beginning of searching, the value of fitness function rises sharply since the first randomly generated values are not bounded. However, the value of cost function falls very fast within few iterations as a result of the updating procedure in PSO algorithm.

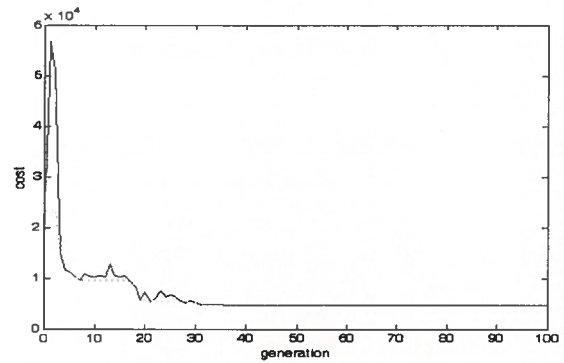


Figure 8. Value of global best of performance index function

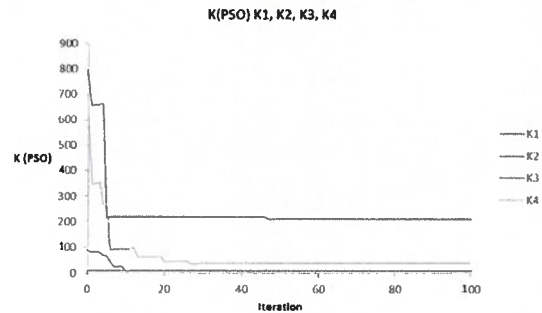


Figure 9. Optimal gains vs iteration

The simulation result of optimal gain  $K$  which provides the minimum value of the performance index function for each iteration is shown in Figure 9. In this figure, the components of the gain arrives the steady state after 48 iterations. The final values of each of the gain components are  $K_1 = 10.2$ ,  $K_2 = 9.9007$ ,  $K_3 = 211.2757$ , and  $K_4 = 37.501$ . This optimal gain results in the minimum value of the performance index function which is around  $0.882 \times 10^4$  as seen in Figure 8.

The results from conventional and proposed LQR techniques for balancing the real inverted pendulum are given in Figures 10 – 12 and Figures 13 – 15, respectively. The comparison of angular displacement from both methods are shown in Figure 10 and Figure 13. It can be seen in these figures that our proposed PSO based LQR provides low average swing compared to traditional LQR, and the maximum swing from the other method is as large as 4 times compared to that from our method. In Figure 11 and Figure 14, the angular velocity results from conventional and our approaches are given, respectively. From these figures, the proposed technique outperforms the other in terms of the overshoot and fluctuation which is as low as 60% of the previous approach. The results of cart position from both methods are given in Figure 12 and Figure 15. As seen in these figures, the results from both methods are almost the same.

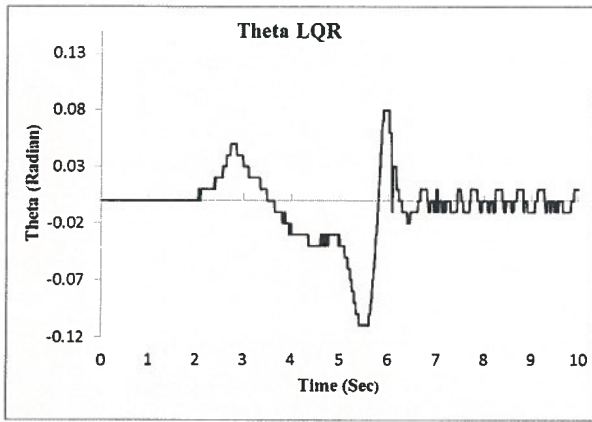


Figure 10. Angular displacement of pendulum obtained from LQR

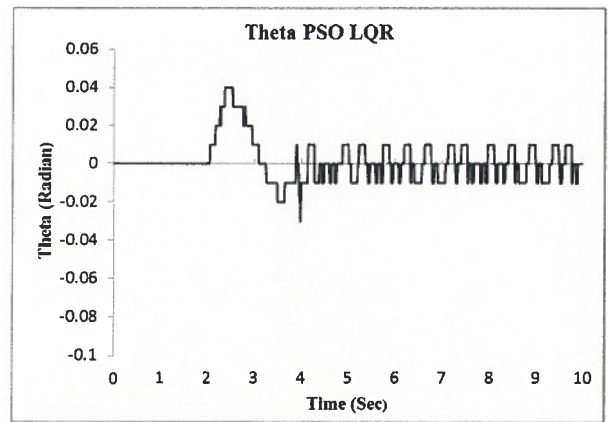


Figure 13. Angular displacement of pendulum obtained from PSO based LQR

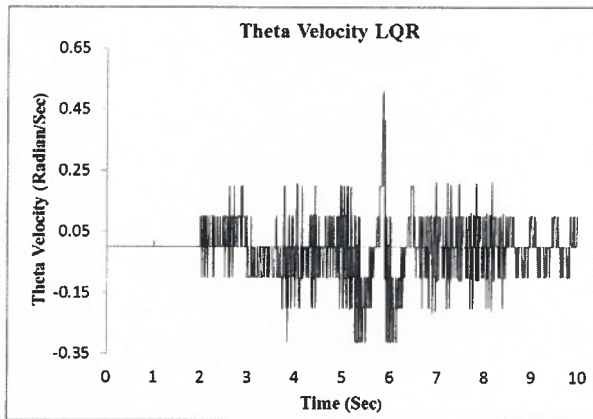


Figure 11. Angular velocity of pendulum obtained from LQR

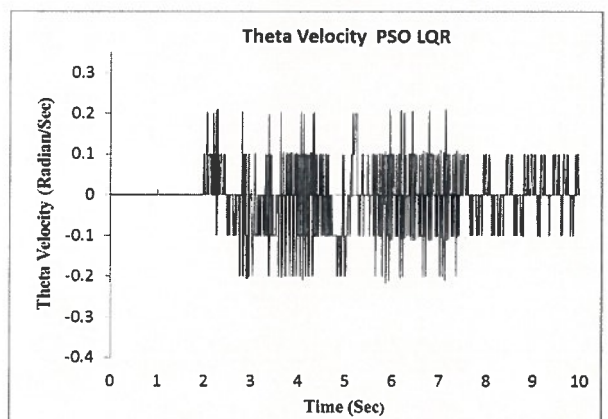


Figure 14. Angular velocity of pendulum obtained from PSO based LQR

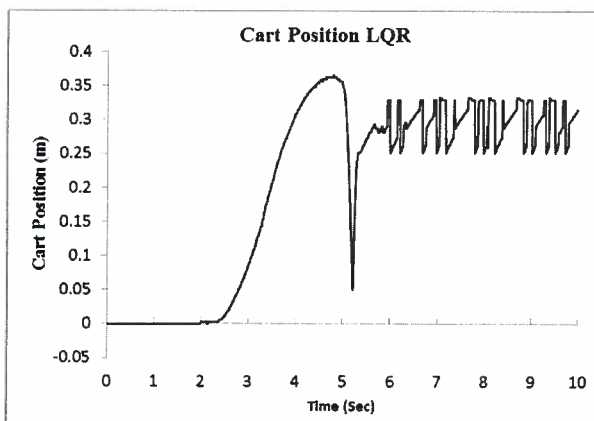


Figure 12. Cart position obtained from LQR

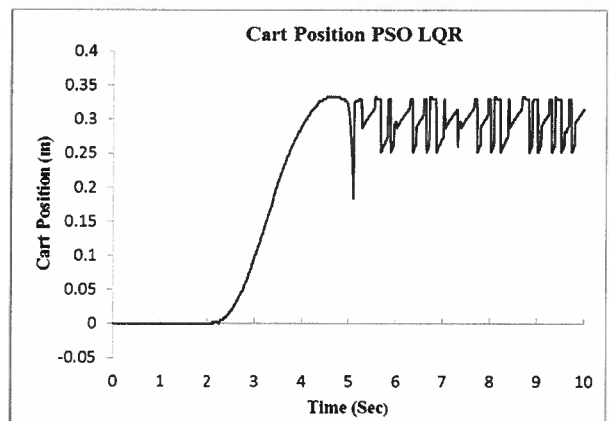


Figure 15. Cart position obtained from PSO based LQR

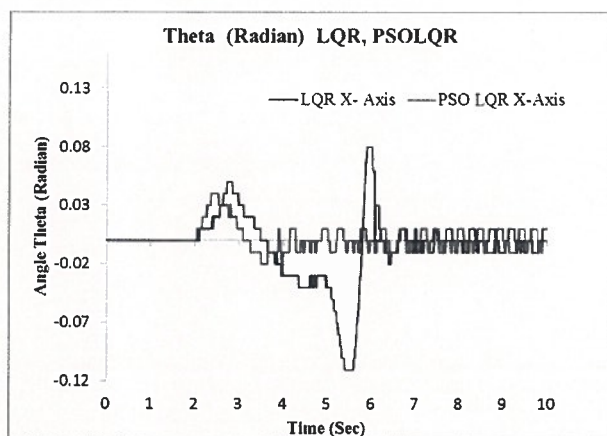


Figure 16. Control performance comparison of PSO based LQR and LQR.

Figure 16 plots the angular displacement results from our proposed PSO based LQR and the conventional methods in the same axis. It is evident in this figure that our proposed method provides better response than the previous technique.

## V. CONCLUSION

This paper introduces a novel technique to balance the single-axis inverted pendulum by use of the proposed PSO based LQR algorithm. In our approach, we use PSO to determine the optimal gain matrix of the LQR controller within finite time duration. The optimal gain result is then evaluated by simulation and real system testing. To assess the proposed method, we directly assign the result of the optimal gain into the instructions of the PLC processor which is used as the main control unit of our physical inverted pendulum. The experimental results show that the proposed method provides better response in term of the swing of the pendulum compared to the conventional LQR approach which fluctuates as large as 4 times of our method.

## REFERENCES

- [1] S. D. Hanwate and Y. V. Hote, "Design of PID controller for inverted pendulum using stability boundary locus," in *Proceedings of the Annual IEEE India Conference (INDICON)*, Pune, India, 2014, pp. 1-6.
- [2] J. X. Xu, Z. Q. Guo and T. H. Lee, "Design and implementation of integral sliding-mode control on an underactuated two-wheeled mobile robot," *IEEE Transactions on Industrial Electronics*, vol. 61, no. 7, pp. 3671-3681, 2014.
- [3] K. Singh, S. Nema and P. K. Padhy, "Modified PSO based PID sliding mode control for inverted pendulum," in *Proceedings of the International Conference on Control, Instrumentation, Communication and Computational Technologies (ICCICCT)*, Kanyakumari, India, 2014, pp. 722-727.
- [4] C. Yang, Z. Li, R. Cui and B. Xu, "Neural Network-Based Motion Control of an Underactuated Wheeled Inverted Pendulum Model," *IEEE Transactions on Neural Networks and Learning Systems*, vol. 25, no. 11, pp. 2004-2016, 2014.
- [5] J. Kennedy, & R. Eberhart, "Particle swarm optimization," in *Proceedings of the IEEE International Conference on Neural Networks*, Perth, WA, 1995, pp. 1942-1948.
- [6] M. Widjaja and S. Yurkovich, "Intelligent control for swing up and balancing of an inverted pendulum system," in *Proceedings of the 4th IEEE Conference on Control Applications*, Albany, NY, 1995, pp. 534-542.
- [7] P. Mason, M. Broucke and B. Piccoli, "Time Optimal Swing-Up of the Planar Pendulum," *IEEE Transactions on Automatic Control*, vol. 53, no. 8, pp. 1876-1886, 2008.
- [8] M. Benedetti, R. Azaro, D. Franceschini and A. Massa, "PSO-Based Real-Time Control of Planar Uniform Circular Arrays," *IEEE Antennas and Wireless Propagation Letters*, vol. 5, no. 1, pp. 545-548, 2006.
- [9] M. Mansouri Borujeni, A. Rashidi and S. M. Saghaeian Nejad, "Optimal four quadrant speed control of switched reluctance motor with torque ripple reduction based on EM-MOPSO," in *Proceedings of the Power Electronics, Drives Systems & Technologies Conference (PEDSTC)*, Tehran, Iran, 2015, pp. 310-315.
- [10] L. B. Palma, F. V. Coito, B. G. Ferreira and P. S. Gil, "PSO based on-line optimization for DC motor speed control," in *Proceedings of the 9th International Conference on Compatibility and Power Electronics (CPE)*, Costa da Caparica, Portugal, 2015, pp. 301-306.
- [11] H. T. Yang, C. T. Yang, C. C. Tsai, G. J. Chen and S. Y. Chen, "Improved PSO based home energy management systems integrated with demand response in a smart grid," in *Proceedings of the 2015 IEEE Congress on Evolutionary Computation (CEC)*, Sendai, Japan, 2015, pp. 275-282.
- [12] H. Yoshida, K. Kawata, Y. Fukuyama, S. Takayama and Y. Nakanishi, "A particle swarm optimization for reactive power and voltage control considering voltage security assessment," *IEEE Transactions on Power Systems*, vol. 15, no. 4, pp. 1232-1239, 2000.